IN VIVO AND IN VITRO CHARACTERIZATION OF DIFFERENT DIMETHYL TRISULFIDE FORMULATIONS

_____

A Thesis

Presented to

The Faculty of the Department Chemistry

Sam Houston State University

_____

In Partial Fulfillment

of the Requirements for the Degree of

Master of Science

_____

by

Christian T. Rios

August, 2020

IN VIVO AND IN VITRO CHARACTERIZATION OF DIFFERENT DIMETHYL TRISULFIDE FORMULATIONS

by

Christian T. Rios

_____

APPROVED:

Ilona Petrikovics, PhD
Committee Director

David E. Thompson, PhD
Committee Member

Tarek M. Trad, PhD
Committee Member

John Pascarella, PhD
Dean, College of Science and Engineering Technology

ABSTRACT

Rios, Christian T., *In vivo and in vitro characterization of different dimethyl trisulfide formulations*. Master of Science (Chemistry), August, 2020, Sam Houston State University, Huntsville, Texas

Cyanide is a toxic cytochrome c oxidase inhibitor that prevents the production of ATP, which consequently results in lactic acidosis, histotoxic hypoxia, and death. Dimethyl trisulfide (DMTS) is a promising sulfur donor (SD) type cyanide antidote that can react with cyanide to form the less toxic thiocyanate. These studies provide more insight into the characterization and biological effects for a newly formulated FF-DMTS compared to Poly80-DMTS.

The first objective was to determine the optimal pH for rhodanese activity. This was determined by observing the SD efficiencies of DMTS and thiosulfate, without rhodanese and comparing that to their activity in the presence of rhodanese at a pH of 7.4, 8.6, and 10.5. Post-reaction, the DMTS (3.5mM) was seen to be over 40x less concentrated than its TS counterpart (150mM), yet exceeds thiosulfate SD ability, supporting the idea that DMTS is a more efficient SD.

Secondly, the *in vitro* blood brain barrier penetrability was determined using a Parallel Artificial Membrane Permeability Assay system. It was determined that the Poly80-DMTS (P_{app} =11.8x10^{-6} cm/s) penetrated the blood brain barrier more than the FF-DMTS (P_{app}=7.46x10^{-6} cm/s), although the Poly80-DMTS (t_{lag}=6.42 min.) had a lag time over 3x longer than FF-DMTS (t_{lag}=2.00 min.).

Thirdly, when analyzing the formation of methemoglobin by DMTS *in vivo*, FF-DMTS produced more methemoglobin than Poly80-DMTS. The highest examined doses

of both formulations, however, produced less than 30% methemoglobin, which is the percentage that would induce methemoglobinemia and require medical assistance.

Lastly, when observing the particle size distribution of the two formulations using the Zetasizer Nano, the particle size of FF-DMTS was almost 3.5x higher than that of the Poly80-DMTS. This can potentially be used to explain the slower blood brian barrier penetrability of FF-DMTS.

The information obtained from these studies will be used for further characterization of DMTS as a cyanide antidote. Understanding how DMTS behaves in the body will give insight into developing an alternative cyanide therapeutic agent. The information from these studies, will contribute to the development of an intramuscular injector kit, which can potentially decrease the lives lost to cyanide intoxication.

KEY WORDS: Cyanide, Sulfur Donor, Dimethyl Trisulfide, Antidote, Rhodanese, Parallel Artificial Membrane Permeability Assay, Blood-Brain Barrier, Particle Size Distribution, PAMPA, Methemoglobin Formation

ACKNOWLEDGEMENTS

First and foremost, I would like to thank Dr. Ilona Petrikovics for her continued support throughout my entire academic career. Without her guidance, I would not have all the opportunities and experience that I have now. I definitely owe a lot of my success to her, and for that, I am very grateful.

Secondly, I would like to thank my committee members, Dr. David Thompson and Dr. Tarek Trad, for their contributions and assistance during my research and thesis writing process.

Next, I would like to thank Dr. Donovan Haines, Mrs. Rachell Haines, and the entire Chemistry Department at Sam Houston State University for providing me with the knowledge, experience, and assistance during my time here at Sam.

Lastly, I would like to thank my family and friends for being there for me throughout this entire process. I definitely could not have done it without their help and support. With this, I would like to give a special thank you to my lab manager Ashley Whiteman and all my fellow lab members for putting up with me and helping me through each phase of this process.

TABLE OF CONTENTS

Page

LIST OF TABLES

LIST OF FIGURES

CHAPTER I

Introduction

Cyanide Toxicity

Cyanide (CN), which represents both CN^- and HCN, is an extremely toxic agent that can cause many detrimental effects after exposure. The severity of these effects is dependent on the concentration of CN that is present within the body. Since CN in the HCN form is a weak acid with a pka value of 9.2, then CN will predominantly exist as HCN at physiologic pH of 7.4.[1] Due to the diminutive structure of the HCN molecule, it can penetrate many biological membranes, such as the blood-brain barrier and mitochondrial membranes. When CN enters the body, it binds to the terminal oxidase of the mitochondrial electron transport chain, also known as the cytochrome c oxidase, which ultimately leads to inhibition of oxygen utilization by the cells and eventually the inhibition of ATP production. When CN is present in the electron transport chain, it binds to the heme iron prosthetic group, Cytochrome a^{2+}. This iron prosthetic group prevents the electrons from flowing from the Cytochrome a^{2+} to the Cytochrome $a_3{}^{3+}$. This inhibition prevents the Cytochrome $a_3{}^{3+}$ from utilizing O_2, which suppresses the body's aerobic metabolic pathway[2]. Figure 1 shows the pathway for CN inhibition of the electron transport chain.

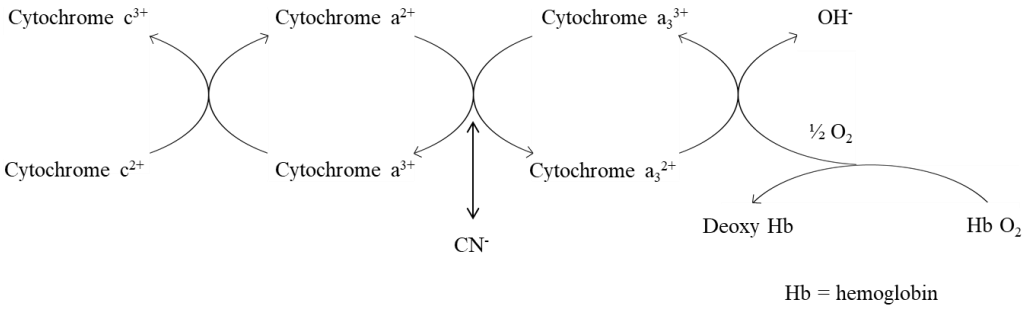

Figure 1. Pathway for Cytochrome C Oxidase Inhibition by CN (reproduced with permission from St. Rosemary Education Institution).

The suppression of the body's aerobic metabolic pathway forces the body to utilize its anaerobic pathway, which causes the reduction of pyruvate to lactic acid, thus leading to lactic acidosis and histotoxic hypoxia.[3]

Cyanide Utilization

Since the 19th century, many countries have utilized CN as a conventional chemical warfare agent. French, Austrian, and German troops were some of the most notorious groups who have utilized CN as a warfare agent in the events such as World War I and II[4] Since then, its use has become more prevalent in contemporary society, especially in cases like the Jonestown Massacre in 1978 and the Tylenol poisonings in 1982. In addition to its use as a chemical warfare agent, CN has many industrial uses as well. CN is a significant factor in the production of many plastics and synthetic rubbers, as well as upholstery and insulations.[3] The use of CN in these industries mean that individuals present during a house fire have a high chance of being exposed to toxic CN. Furthermore, it is also used in mining, electroplating, and chemical research labs.[3]

Current Cyanide Antidotes

Nithiodote™ and Cyanokit® are the two CN antidotes currently available for clinical use in the United States[5]. The active ingredients of Nithiodote™ are sodium nitrite and sodium thiosulfate (TS). Sodium nitrite converts the endogenous hemoglobin (Hb) to methemoglobin (MetHb), which has a high affinity for CN. MetHb proceeds to remove CN from the binuclear heme center of the cytochrome c oxidase and forms cyanomethemoglobin. TS, in the presence of rhodanese (Rh), reacts with CN to form the less toxic metabolite thiocyanate (SCN) that can be easily excreted from the body through urine.[6] The Cyanokit® antidote contains hydroxycobalamin, which contains a cobalt metal center. Since CN has a high affinity to cobalt compounds, the hydroxycobalamin removes the CN from the cytochrome c oxidase and forms cyanocobalamin, which is also excreted from the body through urine.[6] The drawback of these two antidotes is that both must be administered intravenously, which is very inconvenient when treating multiple individuals at once.[7] Therefore, the development of an intramuscular injector kit would allow individuals to treat themselves, which dramatically increases the treatment efficiency for healthcare professionals. This idea is the primary inspiration for this research.

Dimethyl Trisulfide (DMTS)

Sulfane sulfurs and sulfur donors (SD) have been studied as CN antidotes as early as 1894 by S. Lang, where he reported TS as a CN antagonist.[8] He describes how TS can readily combat CN intoxication by converting it to the less toxic SCN, which can be easily excreted through the body via urine. Since then, many other sulfur-containing compounds have been observed as potential CN countermeasures. DMTS is a simple sulfane sulfur

molecule that has become the center of investigation for discovering new CN therapies.[5] DMTS is a naturally occurring compound that can be found in many members of the *Allium* species, such as garlic and onions. DMTS is also responsible for 2.4% of garlic's volatile components.[9] Since members of the *Allium* species contain high amounts of sulfur, they possess a high propensity to serve as adequate SD in CN antagonism. Sulfur has a high affinity for CN and can form the less toxic SCN, which is considered the primary CN detoxifying mechanism in the body. Dr. Petrikovics et al., also observed that DMTS converts CN to SCN over 40 times more efficiently at a pH of 8.6 than that of the current CN antidote Nithiodote™, making DMTS as a potentially efficient CN therapeutic agent.[5]

Rhodanese and Cyanide Reaction

As aforementioned, Rh is a sulfurtransferase enzyme that catalyzes the conversion of CN to the less toxic SCN, due to the transfer of a sulfane sulfur atom. This reaction can be seen in Figure 2 below.

$$CN^- + S_2O_3{}^{2-} \rightarrow SO_3{}^{2-} + SCN^-$$

Figure 2. Conversion of CN to SCN.

The *in vivo* mechanism involves a double displacement reaction in which the sulfur atom of an appropriate SD such as TS (SSO_3^{2-}) reacts with the free enzyme (E) to cleave the disulfide bond and forming a persulfide-substituted enzyme (ES). The ES then can interact with CN, which is a sulfur acceptor substrate to produce SCN.[10] This process can be seen in Figure 3 below.

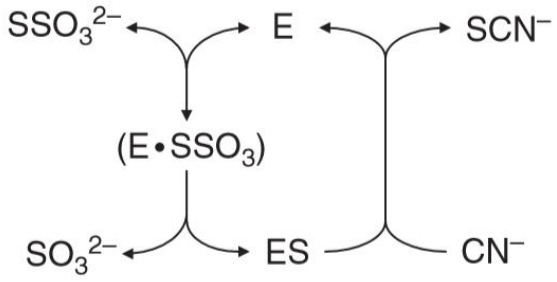

Figure 3. Mechanism of CN to SCN Catalysis by Rh. (Isom, G. E.; Borowitz, J. L.; Mukhopadhyay, S., Sulfurtransferase Enzymes Involved in Cyanide Metabolism. *Comprehensive Toxicology,* **2010***, 485–500.*)

Optimal pH for Rh Activity

The purpose of this experiment is to determine the SD efficacy of DMTS at the optimal pH for Rh activity. In order to do this, a modified version of Sörbo's assay[11] to colorimetrically determine the concentration of thiocyanate was used. The modified method was performed as described by Westley.[12] For this assay, KCN, buffer solution, water, Rh (if used), and TS (or DMTS) and was added into a test tube. These buffers allowed the SD to react with the CN, under a particular pH, in the presence or absence of Rh. The addition of formaldehyde then stopped the reaction from continuing. $Fe(NO_3)_3$ was then added to convert all SCN to $Fe(SCN)^{2+}$. This red iron complex was then measured spectrophotometrically to accurately determine the amount of SCN that was produced.

The Blood-Brain Barrier (BBB)

The BBB is a highly selective semipermeable membrane that divides the blood in the brain from the extracellular fluid of the central nervous system[13]. The BBB regulates the flow of many ions and cells between the blood and the brain. This flow of ions and cells is crucial for the body to maintain homeostasis. Concerning CN, the BBB is also responsible for protecting the neural tissue in the brain from many toxins and pathogens.

Therefore, understanding the many types of pathways across the BBB is essential for the field of drug discovery and delivery.[14] This highly regulated system possesses many routes for transport (Figure 4); however, for this study, the transcellular lipophilic pathway will be the route of interest. Most drugs enter the BBB by transcellular passive diffusion, due to the structure of the tight junctions and the limitations of the other pathways.[15] Since DMTS is a very lipophilic compound, it can easily traverse the BBB through the transcellular lipophilic pathway.

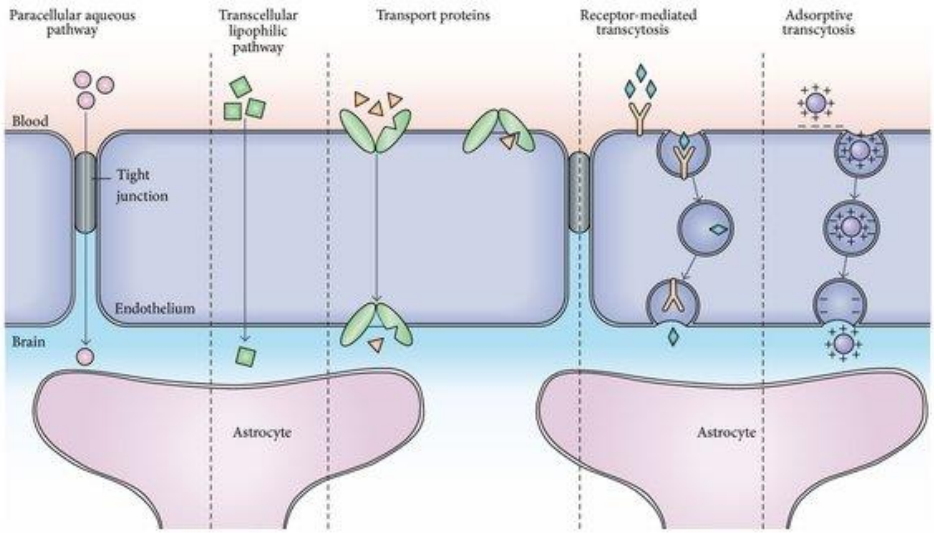

Figure 4. Pathways across the Blood-Brain Barrier (Reprinted by permission from: Springer Nature, Nature Reviews Neuroscience, Astrocyte–endothelial interactions at the blood–brain barrierArticle name, N. Joan Abbott et al, 2006)

Parallel Artificial Membrane Permeability Assay (PAMPA)

This study determines how quickly the various DMTS formulations can cross the BBB. The BBB penetrability of the Poly 80-DMTS formulation has already been determined by Petrikovics's lab.[16] The focus of this particular study was the comparison of

the BBB penetrability by the FF-DMTS formulation to the previously measured Poly 80-DMTS formulation.

The PAMPA system is an artificially created cell membrane system that is widely used in the pharmaceutical industry as a permeability assay.[15] These assays are critical for understanding the absorption of many drugs through various cellular membranes, including the BBB. First introduced by Kansy et al.,[17] the PAMPA system consists of a lower donor plate and an upper acceptor plate. In between these two plates, there is a lipid layer acting as an artificially created membrane layer, which can be seen in Figure 5 below.

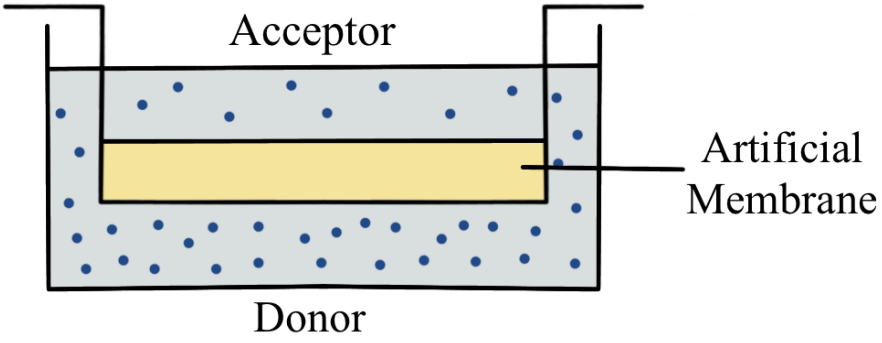

Figure 5. Schematic of PAMPA Model

The artificial membrane is typically formed by impregnating the filter bottom of the PAMPA plate with an organic solvent solution of lipids in order to simulate the cellular membranes of the body.[18] For this particular study, a porcine lipid cocktail was used. Using this lipid cocktail is useful for mimicking the biological environment of the BBB, which allows for the measurement of DMTS penetrability.

Many researchers in the field of drug discovery find the PAMPA system very beneficial due to its low cost, ease of automation, and simplicity. However, the limitations of the PAMPA system are that it only supports passive transport, and fails to emulate both an

active transport pathway and a paracellular pathway.[18] Thus, the PAMPA system can not completely simulate an actual biological membrane.

Particle Size Distribution

The purpose of this experiment is to characterize the particle size distribution of the FF-DMTS formulation in comparison to the previously determined Poly 80-DMTS formulation.[19] Particle size is arguably one of the most important properties of particulate materials.[20] This property is very essential in many industries because understanding the particle characterization can give more insight on a variety of characteristics such as dissolution rates, stability in suspensions, and viscosity. In order to characterize the FF-DMTS formulation via particle size distribution, a Zetasizer Nano series was utilized. This instrument analyzes the sample via a process called dynamic light scattering. Dynamic light scattering, also known as photon correlation spectroscopy, measures the Brownian motion of the solution being analyzed and correlates that to the size of the particles in the solution. Dynamic light scattering is accomplished by directing a helium-neon laser at the sample and analyzing the intensity fluctuations of the scattered light.[21] This scattered light is observed in a process called backscattering detection. For the Zetasizer Nano Series, the application of this process is made by a patented technique called Non-Invasive Back-Scatter (NIBS). Since the backscatter is the property being measured, the laser does not have to go through the entire solution. NIBS minimizes the possibility of scattered light from one particle being scattered by another.[21] This process can be seen in Figure 6.

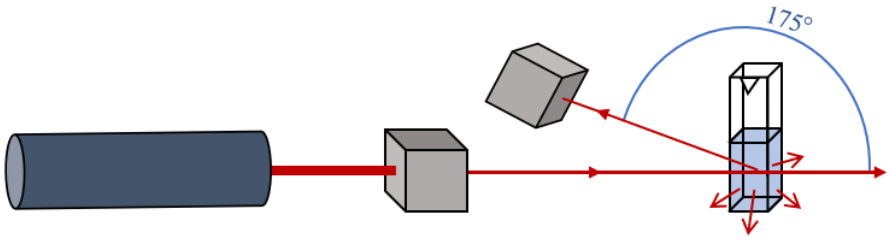

Figure 6. Non-Invasive Back Scatter Detection (Malvern Panalytical, *Zetasizer Nano User Manual*,Malvern Panalytical, 2013. https://www.malvernpanalytical.com/en/learn/knowledge-center/user-manuals/MAN0485EN).

The results from this measurement can be displayed in the form of number, volume, and intensity distributions, seen in Figure 7 below.

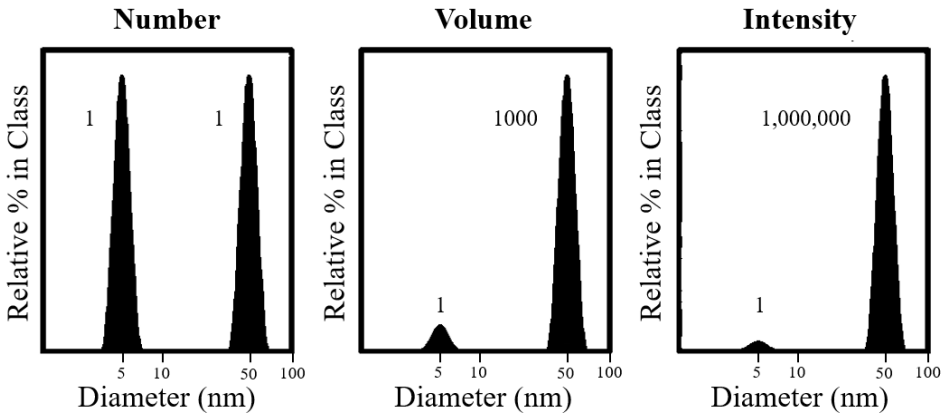

Figure 7. Number, Volume, and Intensity Distributions (Malvern Panalytical, *Zetasizer Nano User Manual*,Malvern Panalytical, 2013. https://www.malvernpanalytical.com/en/learn/knowledge-center/user-manuals/MAN0485EN).

The number distributions display the results as peaks respective to the number of particles of a specific diameter. Volume distributions display the results as peaks respective to the volume of particles of a specific diameter. Lastly, intensity distributions display the results as peaks respective to the amount of light scattered by particles of a specific

diameter. All of these results give insight into the particle distribution and can be used to characterize many particulate materials.

Methemoglobin Formation

Recent studies described the affinity of DMTS to convert Hb to its oxidized form (MetHb*) in vitro*[22] and *in vivo*[23]. In this process, the heme iron center in Hb is oxidized from its ferrous state to a ferric state (Figure 8).

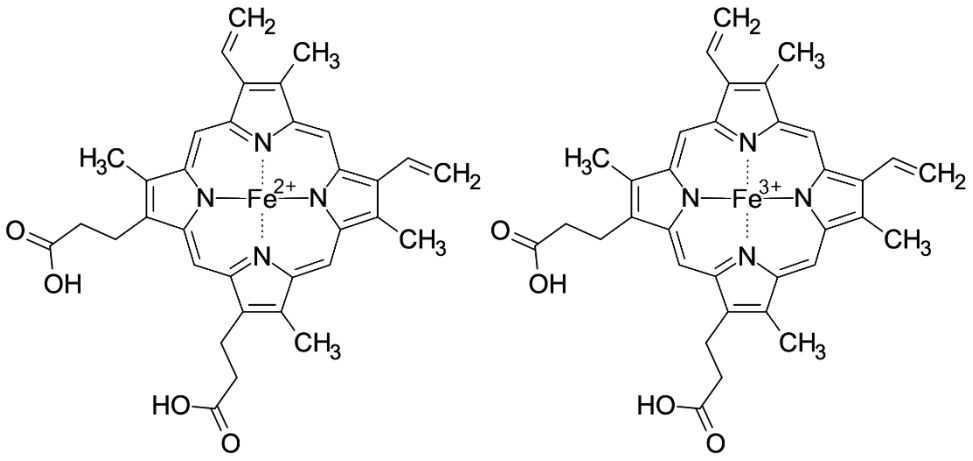

Figure 8. Structure for Hemoglobin and Methemoglobin.(Aintablian, H.; Kabbara, S., Carboxyhemoglobinemia and Methemoglobinemia in an Atypical Case of Salicylate Toxicity: A Potentially Hidden Association, *Exploratory Research and Hypothesis in Medicine*, **2017**, 2(3), 72-76)

Since the ferric state of the oxidized MetHb is unable to bind to oxygen, then this will ultimately hinder the body's ability to transport oxygen to the rest of the body.[24] Although MetHb is unable to bind oxygen, it has a high affinity for CN. Therapeutic agents used to combat CN intoxication, such as Nithiodote^{TM}, take advantage of this phenomenon and purposely induce MetHb formation in the body as a way to combat CN. The purpose of this study is to spectrophotometrically characterize the formation of MetHb by the FF-DMTS formulation *in vivo*, and compare it to the previously published Poly 80-DMTS

formulation.[25] The formation of MetHb by DMTS can potentially offer an alternative route for CN antagonism in addition to DMTS's SD ability.

CHAPTER II

Materials and Methods

Chemicals

The chemicals used in these experiments were DMTS, dimethyl disulfide (DMDS), potassium cyanide (KCN), sodium chloride, sodium hydroxide (NaOH), sodium bicarbonate, ferric nitrate ($FeNO_3$), dimethyl sulfoxide (DMSO), heparin, potassium hexacyanoferrate(III), rhodanese, and 2,4,6-trimethylpyridine were all purchased from Sigma-Aldrich ((Milwaukee, WI, USA). TS, sodium nitrite, poly 80, and hydrochloric acid (HCl) were purchased from Alpha Aesar (Ward Hill, MA, USA). Acetonitrile (ACN), formaldehyde, and water were purchased from VWR (Radnor, PA, USA). Ethanol (EtOH) was purchased from Acros Organics (Thermo Fisher Scientific, Geel, Belgium). Glycine and sodium phosphate monobasic was purchased from JT Baker (Radnor, PA, USA). Prisma HT Buffer, Verapamil, and BSB were purchased from pION (Massachusetts, MA, USA). Sodium biphosphate dibasic were purchased from Thermo Fisher Scientific (Waltham, MA, USA). Isofluorane was purchased from Piramal Enterprises Limited (Telegana, India). FF-DMTS and the FF-solvent was provided by the Southwest Research Institute (San Antonio, TX, USA).

Animals

For *in vivo* and *ex vivo* studies, male CD-1 mice were purchased from Charles River Laboratories (Charles River Laboratories, Inc., Wilmington, Massachusetts, USA). The climate-controlled room that housed the mice had a 12-hour light and a 12-hour dark lighting system and held at a constant temperature of 22℃. The mice were also provided

with water and a 4% Rodent Chow that was purchased from Harlan Laboratories Inc. (Harlan Laboratories Inc., Indianapolis, Indiana, USA). All experiments involving the use of animal models were performed according to the guidelines delineated in the "Guide for the Care and Use of Laboratory Animals" and were performed in a facility accredited by the International Association for Assessment of Laboratory Animal Care (Frederick, Maryland, USA). After each study was completed, the surviving animals were terminated in accordance with the American Veterinary Medical Association Guidelines (American Veterinary Medical Association, Schaumburg, Illinois, USA). The Institutional Animal Care and Use Committee (IACUC) at Sam Houston State University in Huntsville, TX, approved all experiments involving animal models under the IACUC permission number: 15-09-14-1015-3-01.

Instruments

All instruments used in these experiments were located in Dr. Ilona Petrikovics's Lab at Sam Houston State University in Huntsville, TX. Table 1 below, delineates all the instruments used in these experiments as well as their brand and model numbers.

Table 1

Analytical Instruments Employed in this Research

Instrument	Brand	Model Number	Location
HPLC	Thermo Scientific	Dionex Ultimate 3000	Dr. Petrikovics's Lab
GC-MS	Agilent Technologies	7890A / 5975C	Dr. Petrikovics's Lab
Zetasizer Nano	Malvern Panalytical	ZEN3600	Dr. Petrikovics's Lab
PAMPA System	pIon Inc.	FW5024	Dr. Petrikovics's Lab
Genesys Spectrophotometer	Thermo Scientific	GENESYS 10 UV	Dr. Petrikovics's Lab
UV-Vis Scanning Spectrophotometer	Schimadzu	UV-2121	Dr. Petrikovics's Lab
Viscometer	Brookfield Ametek	DV3TLVCJ0	Dr. Petrikovics's Lab

Method for Optimal pH for Rh Activity Determination

For this study, the SD activity of DMTS and TS was observed *in vitro* at three pH levels (7.4, 8.6, and 10.5) in the presence and absence of Rh. For the measurements at different pHs, different buffer solutions were used. The preparation of the different buffers is delineated below.

Preparation of 10 mM Phosphate Buffer Solution (pH=7.4)

This phosphate-buffered saline solution was prepared by weighing 0.238 g of $Na_2HPO_4 \bullet 7\ H_2O$, 0.19 g of $NaH_2PO_4 \bullet 1\ H_2O$, and 8.0 g of NaCl into a 100 mL volumetric flask. DI water was then added just below the line, and the flask was inverted several times to ensure that everything was fully dissolved. Then, more DI was used to fill up the volumetric flask to the line. This solution was then transferred to a VWR glass storage bottle and labeled as "Phosphate Buffer." Using a Thermo Scientific Orion Star A211 pH

meter, a 1 M NaOH solution, and 1 M HCl solution, the pH for this solution was then adjusted to a pH of 7.4.

Preparation of 0.2 M Glycine-NaOH Buffer Solution (pH=8.6)

This glycine-NaOH buffer solution was prepared by weighing out 1.50 g of glycine into a 100 mL volumetric flask. DI water was then added just below the line, and the flask was inverted several times to ensure that everything was fully dissolved. Then, more DI was used to fill up the volumetric flask to the line. This solution was labeled as "Solution A." Next, 0.80 g of NaOH was weighed into another 100 mL volumetric flask and prepared similarly to Solution A. This solution was then labeled as "Solution B." Lastly, 25 mL of Solution A and 22.75 mL of Solution B was added into a third, 100 mL volumetric flask, and dilute to the line with DI water, making the final glycine-NaOH buffer solution. This solution was then transferred to a VWR glass storage bottle and labeled as "Glycine-NaOH Buffer." Using a Thermo Scientific Orion Star A211 pH meter, NaOH solution (1M), or HCl solution (1M), the pH for this solution was then adjusted to a pH of 8.6.

Preparation of 0.2 M Carbonate Buffer Solution (pH=10.5)

To make this carbonate buffer, 0.84 g of $NaHCO_3$ was weighed into a 100 mL volumetric flask and prepared as aforementioned. This solution was labeled as "Solution C." Next, 2.86 g of anhydrous Na_2CO_3 was weighed into another 100 mL volumetric flask and also prepared as aforementioned. This solution was then labeled "Solution D." Lastly, 20 mL of Solution C and 80 mL of Solution D was added into a VWR glass storage bottle and labeled as "Carbonate Buffer." Using a Thermo Scientific Orion Star A211 pH meter,

NaOH solution (1M), or HCl solution (1M), the pH for this solution was then adjusted to a pH of 10.5.

Preparation of 100 U/mL Rh Solutions

To make the Rh solutions, 1 mg (100 U/mg) of Rh was weighed into three 1.5 mL amber Eppendorf tubes. Into one tube, 1 mL of the phosphate buffer (pH=7.4) was added. This solution was then hand vortexed until fully dissolved and labeled appropriately. This process was then repeated for the glycine-NaOH (pH=8.6) buffer and the carbonate (pH=10.5) buffer and stored at 4℃.

To begin the experiment, the following solutions were added sequentially into a 16x125 mm test tube:

1. 390 µL of DI water
2. 200 µL of buffer solution
3. 10 µL Rh or DI water
4. 200 µL of SD (3.5 mM DMTS, 150 mM TS, or neither)
5. 200 µL of 250 mM KCN

Total volume: 1000 µL.

For the measurement of the blank, the addition of a SD was excluded and replaced by DI water. Once the solutions were pipetted, the test tubes were sealed by using Parafilm, hand vortexed for 10 seconds, and incubated at room temperature for one minute. Immediately after the one minute incubation period, the following solutions were added to the test tube:

1. 500 µL of a 15% formaldehyde solution
2. 1500 µL of 40 mM $Fe(NO_3)_3$ solution

Once these solutions were added, they were again sealed with Parafilm and hand vortexed for 10 seconds. After being hand vortexed, 1000 µL of the final solution was measured spectrophotometrically at 460 nm using a plastic polystyrene (PS) cuvette.

Figure 9 shows a schematic of this procedure.

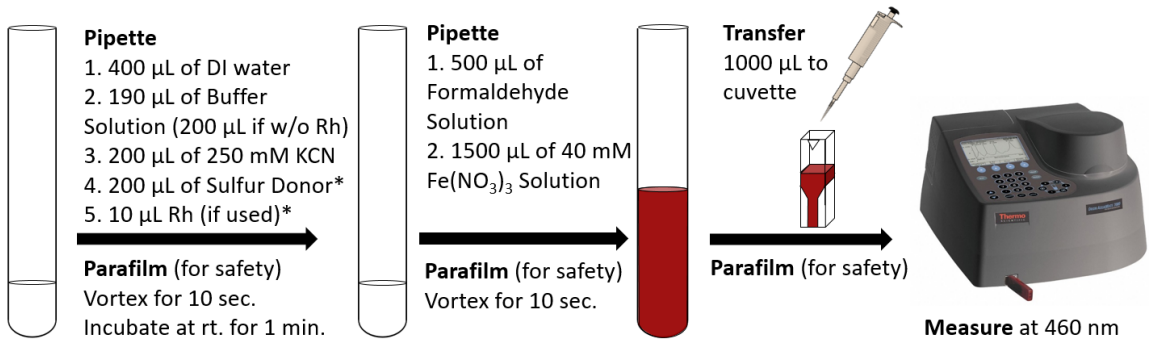

Figure 9. Detailed Schematic of the Rh Study Protocol

$Fe(SCN)^{2+}$ Calibration Curve

To create a calibration curve for $Fe(SCN)^{2+}$, twelve caliber solutions were prepared, ranging between 0.0 mM - 2.0 mM $Fe(SCN)^{2+}$. In order to prepare these calibers, a 0.25 M $Fe(SCN)^{2+}$ was made by combining a 0.5 M $Fe(NO_3)_3$ solution, and a 1.5 M KSCN solution. These solutions were prepared as follows:

Preparation of a 0.5 M $Fe(NO_3)_3$ Solution

Into a 10 mL volumetric flask, 1.210 g of $Fe(NO_3)_3 \bullet 9\ H_2O$ was added and filled to the marked line with DI water. This solution was then inverted several times until it was completely dissolved.

Preparation of a 1.5 M KSCN Solution

Similarly, to the previous solution, 1.460 g of KSCN weighed out and placed into a 10 mL volumetric flask. This solution was then diluted to the mark using DI water. The flask was then inverted several times until fully dissolved.

Preparation of a 0.25 M $Fe(SCN)^{2+}$ Solution

To prepare this solution, 10 mL of the 0.5 M $Fe(NO_3)_3$ solution and 10 mL of the 1.5 KSCN solution were added to a 20 mL glass vial. This vial was then capped and hand vortexed for one minute.

Preparation of a 2.5 mM $Fe(SCN)^{2+}$ Stock Solution

To prepare this solution, 200 µL of the 0.25 M $Fe(NO_3)_3$ solution and 19.8 mL of DI water were added to a 20 mL glass vial. This vial was then capped and hand vortexed for one minute or until fully mixed. After using the hand vortex, the vial was then labeled appropriately. This solution was then used to prepare the twelve caliber solutions.

Preparation of Twelve Caliber Solutions

Using the previously made 2.5 mM $Fe(NO_3)_3$ Stock Solution, twelve caliber solutions were made into 1.5 mL plastic PS cuvettes with concentrations of 0, 0.005, 0.025, 0.05, 0.10, 0.25, 0.50, 0.75, 1.0, 1.25, 1.50, 1.75, and 2.0 mM. These solutions were made by using the dilution equation below, where C_1 is the initial concentration of 2.5 mM $Fe(NO_3)_3$, V_1 is the volume (µL) of stock solution needed, C_2 is the target concentration, and V_2 is the final volume of 1000 µL.

$$C_1V_1 = C_2V_2$$

Figure 9. Dilution Equation

Once all the twelve caliber solutions were made, they were measured spectrophotometrically at 460 nm and used to create a calibration curve. For these measurements, 1000 µL of DI water was used as blank.

Method for BBB Penetration by FF-DMTS and Poly 80-DMTS

For this PAMPA method, the 96-well polyvinylidene membrane microplates with pre-loaded magnetic stirrers were impregnated with 2% porcine brain lipid following the instructions delineated in the Pion PAMPA Instruction Manual (REF). For the PAMPA study using the FF-DMTS formulation, 90 µL of the 10 mg/mL FF-DMTS stock solution was diluted with 8.91 mL of diluted Prisma HT Buffer. This Prisma HT Buffer solution was previously set to a pH of 7.4 using 1.0 M NaOH and a Thermo Scientific Orion Star A211 pH meter. 180 µL of the resulting 0.1 mg/mL FF-DMTS in Prisma HT Buffer solution was pipetted into three wells on the donor plate. Following this, the acceptor plate was carefully mounted onto the donor plate, ensuring that no air gets in between the donor plate and the lipid membrane on the acceptor plate. Then, 200 µL of the FF-DMTS in Brain Sink Buffer (BSB) solution was pipetted into the corresponding acceptor wells. This FF-DMTS-BSB solution was prepared by diluting 200 µL of the vehicle for FF-DMTS (FF-solvent) with 19.8 mL of BSB concentrate. Once the FF-DMTS-BSB solution was pipetted into the acceptor plate, it was then sealed using the PAMPA sealing tape. The PAMPA sandwich was then carefully placed into the GutBox, the thickness of the aqueous boundary layer was set to 40 µm, and the sponges were saturated with deionized water. The GutBox was then turned on, and the PAMPA plate was allowed to incubate for a total of 90 minutes. Once the GutBox was started, 200 µL of the solution was extracted from the acceptor plate every 30 minutes. After each extraction, 200 µL of the FF-solvent was then pipetted back into the acceptor plate. The extracted samples were then analyzed using the HPLC.

To prepare the solutions for HPLC analysis, glass inserts were first placed into HPLC vials. Then, 60 µL of a 0.05 mg/mL DMDS in ACN solution was then pipetted into

the first insert along with 40 µL of the extracted solution. This vial was then sealed and placed into the HPLC for analysis. These same steps were repeated for the 0, 30, 60, and 90-minute samples.

Table 2

Donor and Acceptor Sample Collection Times for PAMPA

Donor		Acceptor	
Sample	Sample collection time (min)	Sample	Sample collection time (min)
100 µg/mL DMTS and FF solvent in Prisma HT buffer	0, 90	Brain Sink Buffer Solution + FF solvent	30, 60, 90
50 µM Verapamil in DMSO + FF solvent (Solution in Prisma HT buffer)	0, 90	Brain Sink Buffer Solution + FF solvent	90
50 µM Verapamil in DMSO in Prisma HT buffer	0, 90	Brain Sink Buffer "Concentrate"	90

Method for Particle Size Distribution Comparison of FF-DMTS and Poly 80-DMTS

For this experiment, the Poly 80-DMTS formulation (50 mg DMTS /15% Poly80 mL) was prepared according to the protocol patented by the Petrikovics's lab (US20150297535, 2015).

Preparation of the 15% Poly 80 Solution

Using an analytical balance, 3 g of Poly 80 was pipetted into a 20 mL glass vial. To this vial, HPLC-grade water was added until the scale read 20 g. A stir bar was then added to the vial, and the vial was sealed using a rubber cap. This vial was then allowed to stir for approximately 30 minutes. After the 30 minutes, the solution was crimp sealed and

hand-shaken until the Poly 80 was fully dissolved. Once it was fully dissolved, the vial was labeled appropriately and stored at 4 °C overnight.

Preparation of the 50 mg/mL DMTS in 15% Poly 80 Solution

The previously prepared 15% Poly 80 solution was removed from the fridge and left at room temperature for approximately 30 minutes. To prepare the 50 mg/mL DMTS solution, 500 mg of DMTS was pipetted into a 10 mL volumetric flask. Then, the 15% Poly 80 solution was added to the volumetric flask until it reached the marked line. The volumetric flask was capped and hand vortexed for approximately 5 minutes. The solution was transferred to a 10 mL glass vial and crimp sealed. This solution was then auto vortexed at maximum speed for approximately 30 minutes, followed by handshaking for another 10 minutes. Once that was completed, the vial was labeled appropriately and stored at 4 °C overnight.

To run this experiment, the Zetasizer Nano was turned on and allowed to warm up for approximately one hour. Then, the Standard Operating Procedure (SOP) parameters for the measurement of the Poly 80-DMTS solution and the FF-DMTS solution were each created using the following method. Under the “Sample” tab, the sample name and any notes were listed. Below this tab, there was the “Material” tab. This section is where DMTS, which has a refractive index of 1.602 and an absorption value of 0.001, was entered. Next, the Dispersant for the Poly 80-DMTS formulation was selected to be the 15% Poly 80 Solution. Since the temperature, viscosity, and refractive index were needed for this portion, 25 °C, 2.270, and 1.350 were entered, respectively. Alternatively, for the Dispersant for the FF-DMTS formulation, the 10% Aqueous Vehicle was selected. Instead of the values listed before, this Dispersant has a temperature of 25 °C, a viscosity of 0.620,

and a refractive index of 1.367. Once the values of the Dispersant were entered, the Temperature and Equilibration time was entered as 25 °C for 30 seconds in the "Temperature" tab. Lastly, Under the "Measurement" tab, a 173° Backscatter was selected as the measurement angle with three measurements and 0 seconds between each measurement. All other parameters remained unaltered from the default settings.

After the SOP for each sample measurement was loaded, 1000 µL of the sample was pipetted into a PS cuvette so that the sample depth remained between 10 mm and 15 mm from the bottom of the cuvette. The cuvette was then placed into the sample compartment and measured.

Method for *In Vivo* Methemoglobin (MetHb) Formation by DMTS Formulations

Prior to the start of this experiment, the following solutions were prepared: 500 U/mL heparin solution, 5% (m/v) $K_3Fe(CN)_6$, 0.675% (v/v) Colloidine Buffer, and a 5% (m/v) KCN. A detailed protocol for the preparation of these solutions can be seen below:

500 U/mL Heparin Solution

Using an analytical scale, 13.85 mg of heparin was added to a 5 mL glass vial. To this, 5 mL of DI water was added, and the vial was crimp sealed. The sealed vial was then left on the auto vortex at max speed until heparin was fully dissolved. This solution was then labeled and kept at 4°C until further use.

5% (m/v) $K_3Fe(CN)_6$ Solution

Using an analytical scale, 250 mg of solid $K_3Fe(CN)_6$ was added to a 5 mL glass vial. To this, 5 mL of DI water was added, and the vial was crimp sealed. The sealed vial

was wrapped in foil and left on the auto vortex at max speed until everything was fully dissolved. This solution was labeled and kept at room temperature until further use.

0.675% (v/v) Colloidine Buffer Solution

Into a 500 mL volumetric flask, approximately 400 mL of sonicated DI water was added. To this, 3.375 mL of 2,4,6-trimethylpyridine and 1.75 mL of HCl was added. Then, using more DI water, the flask was filled until the meniscus reached the marked line. This solution was inverted several times until fully mixed and transferred to a VWR glass storage container. This solution was then labeled and kept at 4°C until further use.

5% (m/v) KCN Solution

The preparation of the KCN solution was done completely under a fume hood to ensure proper safety protocols. Also, the wearing of thick rubber gloves, goggles, and a lab coat was strictly enforced for this preparation. First, the desiccator containing the solid KCN salt was brought into the fume hood as well as the analytical scale and the hand vortex. Then, 1.250 g of the KCN salt was weighed and added into a 25 mL volumetric flask. To this flask, 25 mL of DI water was added until the meniscus reached the marked line. The flask was then capped, sealed with Parafilm, and hand vortexed until the KCN was fully dissolved. Once dissolved, the KCN solution was transferred into three, 10 mL glass vials and crimp sealed. These solutions were then labeled and kept at room temperature until further use.

Mice Injection by the FF-DMTS Formulation

These animal studies were conducted in accordance with the guidelines of The Guide for the Care and Use of Laboratory Animals (National Research Council, 2010),

accredited by AAALAC (American Association for the Assessment and Accreditation of Laboratory Animal Care, International). At the end of the experiment, all remaining animals were euthanized in accordance with the AVMA Guidelines for the Euthanasia of Animals: 2013 Edition (AVMA Guidelines). The Institutional Animal Care and Use Committee (IACUC) permission number is 15-09-14-1015-3-01.

Once these solutions were prepared, a pre-weighed CD-1 male mouse was then injected with the FF-DMTS formulation into the right thigh muscle. The injection volume was calculated using the following equation below.

$$\text{Injection Volume } (\mu L) = \frac{dose\ \left(\frac{mg}{kg}\right) * weight\ (g)}{stock\ solution\ concentration\ (\frac{mg}{mL})}$$

Figure 10. Equation Used to Calculate Injection Volume.

When the injection volumes exceeded the 50 µL injection per injection site limit, the solution was divided and was injected into two legs. After injection, the mice were allowed to incubate for their designated incubation times. Approximately 4 minutes before the end of the incubation period, the mice were anesthetized using isoflurane, and their chest cavity was exposed. Once the incubation period was complete, blood was drawn directly from their heart, using a heparinized syringe, and transferred to a heparinized 5 mL glass vial. 0.2 mL of this blood was transferred to a 10 mL glass vial, and 5 mL of DI water was added. This solution was auto vortexed for 1 minute at 2000 RPM. To this, 5 mL of the 0.675% (v/v) colloidine buffer was added, and the solution was auto vortexed again. This solution was then transferred into nine different 1.5 mL amber Eppendorf tubes and centrifuged for three minutes at 4 °C and 10000g. The supernatant from these vials was collected into a single 20 mL glass test tube. 4.8 mL of this supernatant collection was then

pipetted into two separate 10 mL glass test tubes. To test tube1, 50 µL of the 5% (m/v) $K_3Fe(CN)_6$ solution was added, and to the test tube 2, 50 µL of DI water was added. These test tubes were then mixed thoroughly. Using a 1000 µL pipette, each test tube was divided evenly into two 3 mL plastic PS cuvettes. Into two cuvettes (one from the 5% (m/v) $K_3Fe(CN)_6$ test tube and one from the DI water test tube), 50 µL of DI water was added. To the remaining two test cuvettes, 50 µL of the 5% KCN solution was added. Immediately after each addition, the cuvettes were covered with Parafilm, mixed by inversion for about five times, and left to incubate at room temperature for 5 minutes. After the incubation period, the absorbance of each cuvette was measured spectrophotometrically at 630 nm. A detailed figure of this procedure can be seen in the Appendix.

CHAPTER III

Results and Discussion

Optimal pH for Rh Activity Determination

In order to determine the optimal pH for Rh activity, SDs TS and DMTS were monitored *in vitro* at a pH of 7.4, 8.6, and 10.5 with and without Rh. These specific pH values were tested since 7.4 is the physiological pH of the human body, and pHs 8.6 and 10.5 have been reported to be the optimal pH for Rh activity.[11,26,27]

To observe the enzymatic conversion of CN to SCN at all pH values, the three different buffers were used with Rh. To observe the spontaneous conversion of CN to SCN, the 7.4 Glycine-NaOH buffer was used without Rh. Using a concentration of 150 mM TS and 3.5 mM DMTS, the correlation between TS and DMTS SD activity both in the presence and absence of Rh was determined.

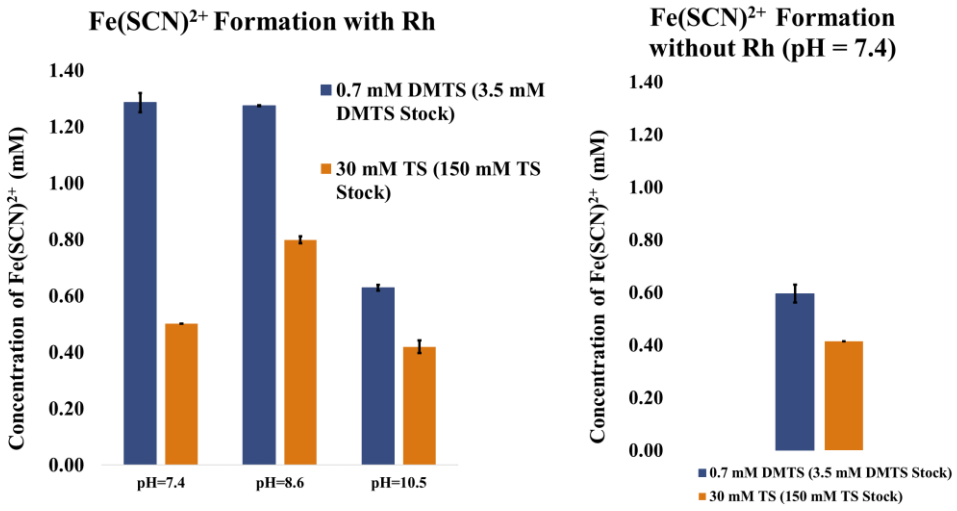

Figure 11. $Fe(SCN)^{2+}$ Formation with Rh (left) and without Rh (right) with SDs DMTS and TS. Note: Concentrations for SDs represent the total concentration in solution after being diluted from their stock concentrations.

After the SDs were able to react with the CN to form SCN, they were then treated with $Fe(NO_3)_3$ to form the metal complex $Fe(SCN)^{2+}$. This metal complex was measured spectrophotometrically at 460 nm to determine the amount of SCN formed.

It can be seen in Figure 11 that DMTS produced more SCN than TS, both in the presence and absence of Rh. For Rh at pHs of 7.4, 8.6, and 10.5, the concentrations of $Fe(SCN)^{2+}$ produced from the 3.5 mM DMTS solution were approximately 1.30, 1.30, and 0.60 mM, respectively. For TS, the concentrations of $Fe(SCN)^{2+}$ was significantly lower. For Rh at pHs 7.4, 8.6, and 10.5, the concentrations of $Fe(SCN)^{2+}$ from 150 mM TS were 0.50, 0.80, and 0.40 mM, respectively. Without Rh, tested at a pH of 7.4, the 3.5 mM DMTS solution produced approximately 0.60 mM of $Fe(SCN)^{2+}$, and the 150 mM TS solution produced approximately 0.40 mM of $Fe(SCN)^{2+}$.

More importantly, the concentration of DMTS can be seen to be over 40 times less concentrated than its TS counterpart. This supports the idea that DMTS is a much more efficient SD than TS. In the case of the optimal pH for Rh activity, it can be seen that SCN is produced in the highest concentrations at a pH of 8.6 for DMTS and TS. Although the SCN formation for DMTS is comparable at a pH of 7.4 and 8.6, this can be attributed to the spontaneous formation of SCN without the use of the sulfurtransferase enzyme. In the case of TS, SCN concentrations reached a maximum at a pH of 8.6. These concentrations can be attributed to TS's dependence on Rh for the conversion of CN to form SCN. Since SCN concentrations reached a maximum at the pH of 8.6, it suggests that the optimum pH for Rh activity is near 8.6.

To further support these claims, a calibration curve using SCN at concentrations of 0, 0.50, 0.58, 0.67, 0.75, 0.92, 1.00, and 1.04 mM was created. For this calibration curve,

the data is represented as an average of three measurements with their corresponding standard deviations. Some error bars may not be visible due to their very low standard deviation.

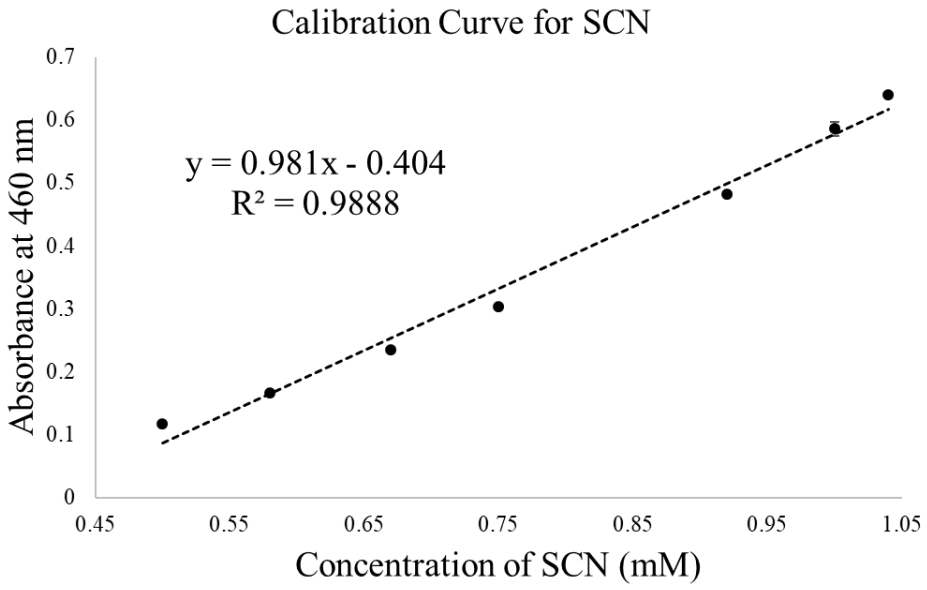

Figure 12. Calibration Curve for SCN at 460 nm.

The resulting calibration curve (Figure 12) shows a linear plot with an R^2 of 0.9888 and an equation of y = 0.981x-0.404. For this calibration curve, the limit of detection (LOD) and the limit of quantitation (LOQ) were determined using the equations below.

LOD = 3s / m = (3 × 0.0029) / 0.981 = 0.009 mM

LOQ = 10s / m = (10 × 0.0029) / 0.981 = 0.029 mM

For these calculations, m is the slope and s is the standard deviation of the least concentrated caliber solution, which was calculated using the equation below.

$$s = \sqrt{\frac{\sum(x_m - x_i)^2}{n-1}}$$

In addition, the accuracy and precision percentage values were also calculated using the equations below:

$$Accuracy\ (\%) = \frac{x_{\ predicted} - x_{\ measured}}{x_{\ measured}} * \ 100$$

$$Precision\ (\%) = \frac{Standard\ deviation\ of\ absorbance}{Mean\ absorbance} * \ 100$$

Figure 13. Equations Used to Calculate Accuracy and Precision.

The calculated values for accuracy and precision can be seen in Table 3.

Table 3

Accuracy and Precision for SCN Calibration Curve

[SCN] (mM)	Accuracy (%)	Precision (%)
0.50	-5.7	2.5
0.58	-0.2	1.4
0.67	3.0	0.9
0.75	4.0	0.7
0.92	1.8	2.3
1.00	-0.9	0.4
1.04	-2.0	0.8

Blood-Brain Barrier Penetration by FF-DMTS and Poly 80-DMTS

The PAMPA system is a widely used method that measures the membrane penetration of various drugs through a model membrane. For this experiment, the clearance volume (C_{vol}), lag time (t_{lag}), and the apparent permeability (P_{app}) of the FF-DMTS formulation were determined and compared to the values obtained previously for the Poly 80-DMTS formulation.[16]

Understanding the C_{vol}, which can be defined as the amount of DMTS filtered out of the blood and into the BBB over time, can be highly advantageous in the analysis of transmembrane diffusion. For this study, the C_{vol} of the FF-DMTS formulation was determined at the time intervals of 30, 60, and 90 minutes (Figure 4). Compared to the Poly 80-DMTS formulation, which had an average C_{vol} of 4.998, 11.358, and 17.718 µL for the respective 30, 60, and 90-minute time points, the FF-DMTS formulation had a relatively slower clearance rate (Table 4).

Table 4

Clearance of FF-DMTS

Time (min.)	C_{vol} (µL)	Average	Standard Deviation
30	4.16	3.46	1.18
	2.26		
	3.96		
60	9.11	7.44	1.57
	5.99		
	7.22		
90	14.79	11.28	3.05
	9.74		
	9.32		

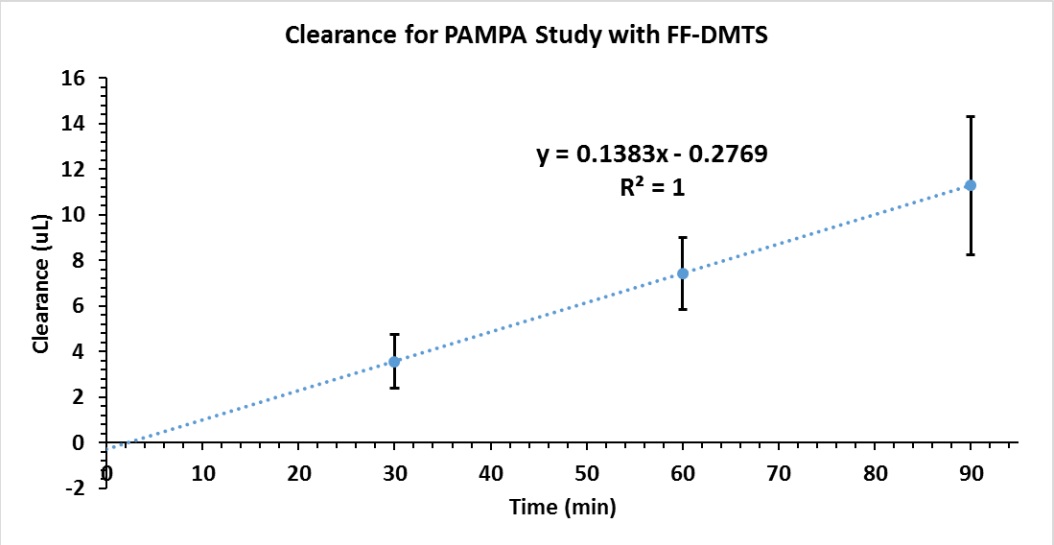

Figure 14. Clearance for PAMPA Study with FF-DMTS. Each data point represents the average of three measurements plus or minus the standard deviation (n=3)

Based on this information, the t_{lag} for the FF-DMTS formulation was determined to be 2.00 minutes. The t_{lag} is defined as the finite time taken for DMTS to appear within the acceptor portion of the PAMPA plate.[17] Compared to the t_{lag} of the Poly 80-DMTS formulation, which has a t_{lag} of 6.42 minutes, the FF-DMTS appears in the acceptor plate nearly three times quicker.

Lastly, the Poly 80-DMTS formulation was found to have a P_{app} of 11.8×10^{-6} cm/s. Based on these experiments, the P_{app} for FF-DMTS was found to be 7.46×10^{-6} cm/s, which is six times lower than that of the Poly 80-DMTS formulation.

The P_{app} was calculated using the equation below.

$$P_{app} = \frac{Volume\ of\ acceptor(mL) * Concentration\ of\ acceptor_{\Delta t}(\frac{\mu g}{mL})}{area\ of\ the\ filter\ (cm^2) * time\ (s) * Concentration\ of\ donor_{t_0}\ (\frac{\mu g}{mL})}$$

Figure 15. Equation Used to Calculate Apparent Permeability.

The P_{app} of each triplicate measurement was calculated using this equation, and the reported P_{app} represents the average of each P_{app} value. The standard deviation for this was determined to be $2.25x10^{-6}$ cm/s. To obtain the values for the concentration of DMTS in the acceptor plate, which was needed for P_{app} calculations, a calibration curve (Figure 16) was created. For this calibration curve, DMDS was used as an internal standard. Values for c_{vol} for the FF-DMTS formulation are denoted as an average plus minus the standard deviation (n=3). The standard deviation for the Poly 80-DMTS formulation was not provided by the article. Table 5 shows a summary of the data found using these experiments.

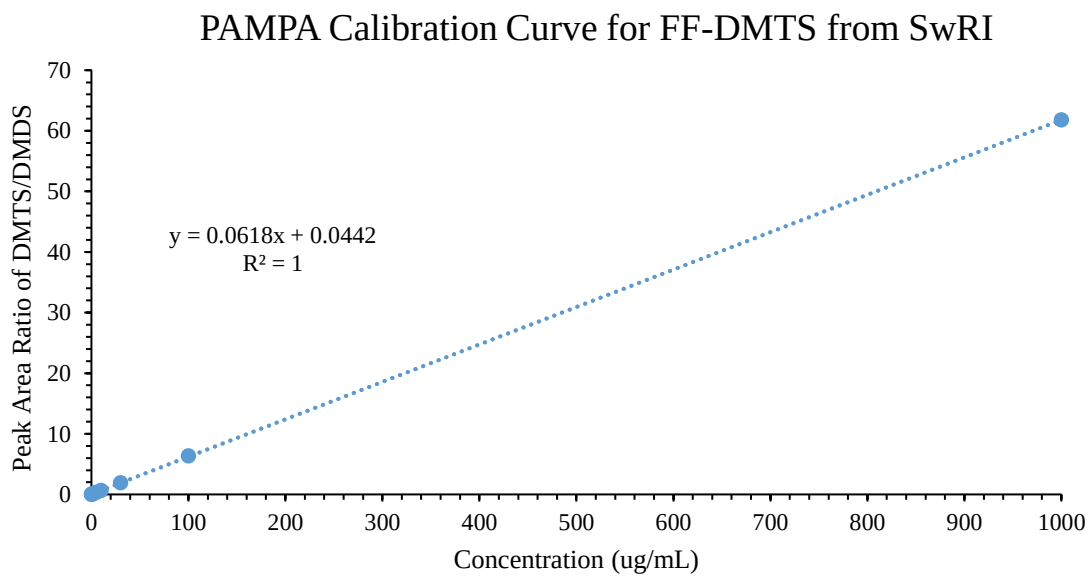

Figure 16. PAMPA Calibration Curve for FF-DMTS.

Table 5

Clearance Volume, Lag Time, and Apparent Permeability of FF-DMTS and Poly 80-DMTS Formulations

	Poly 80-DMTS*	FF-DMTS
Clearance Volume (C_{vol})		
30 minutes	5.0 µL/min	3.6 ± 1.2 µL/min
60 minutes	11.0 µL/min	7.4 ± 1.6 µL/min
90 minutes	18.0 µL/min	11.0 ± 3.0 µL/min
Lag Time (t_{lag})	2.05 min.	2.00 min.
Apparent Permeability (P_{app})	12.0×10^{-6} cm/s	7.5×10^{-6} cm/s

*Note. Values for C_{vol} are denoted as averages (n=3). *Standard deviations for Poly 80-DMTS were not provided from the reference article[16].*

Particle Size Distribution Comparison of FF-DMTS and Poly 80-DMTS

Based on the volume distributions for the FF-DMTS formulation and the Poly 80-DMTS formulation, the particle size of the FF-DMTS is over 3.5x higher than that of the Poly 80-DMTS formulation. For the Poly 80-DMTS formulation, a particle size with a diameter of 4.275 nm contributed to 100% of the light scattered. Conversely, for the FF-DMTS formulation, a particle size with a diameter of 15.77 nm contributed to 99.0% of the total light scattered. Based on these volume distributions, we can determine that the FF-DMTS formulation produces bigger micelles compared to the Poly 80-DMTS formulation, which can explain why the Poly 80-DMTS formulation has a higher P_{app} than the FF-DMTS formulation.

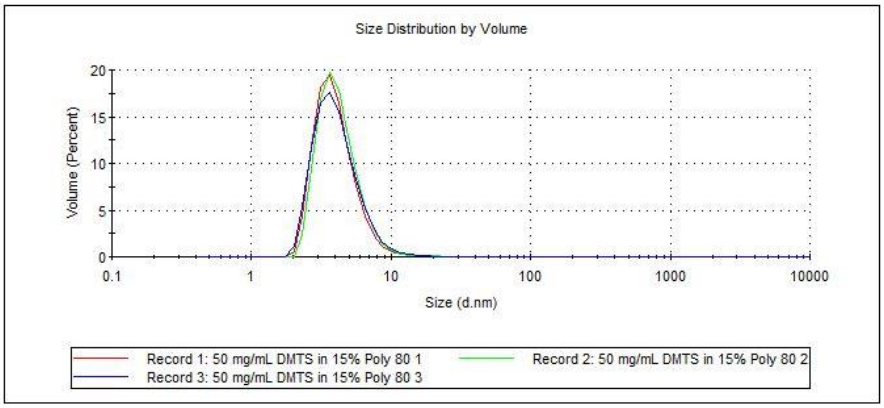

Figure 17. Size Distribution by Volume for 50 mg/mL Poly 80-DMTS formulation.

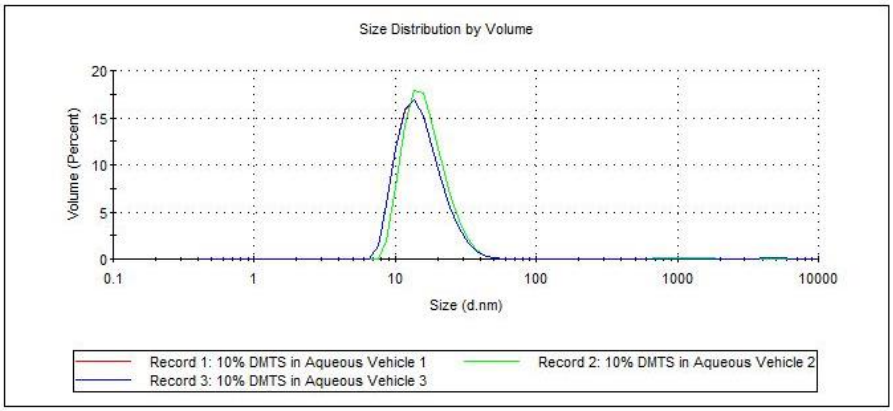

Figure 18. Size Distribution by Intensity for 100 mg/mL FF-DMTS formulation.

In Vivo Methemoglobin Formation by DMTS Formulations

The purpose of this study is to characterize the *in vivo* MetHb formation by the FF-DMTS *in vivo* on a mice model and compare it to the results of the previously published Poly 80-DMTS formulation.[22] Recent experiments show the relationship between the DMTS dose and MetHb formation. The FF-DMTS formulation was injected via intramuscular injection (IM) into CD-1 male mice (15-30 g) at several doses and sampling times. The doses applied were 25, 100, 175, 220, 277, and 349 mg/kg with sampling times of 5, 10, 20, 30, and 60 minutes.

The data sets for MetHb formation were split into two sets: a low dose, and a high dose. The "low dose" data set (Figure 19) includes doses of 25, 100, and 175 mg/kg which were injected into one leg, while the "high dose" data set (Figure 20) consisted of doses 220, 277, and 349 mg/kg, which were injected into two legs.

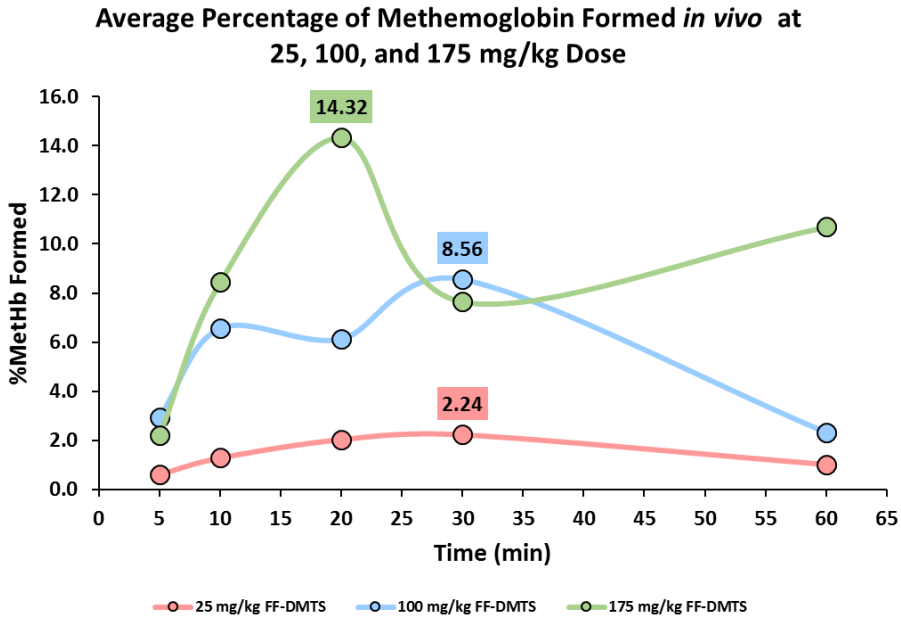

Figure 19. "Low Dose" Data Set for MetHb Formation after IM Injection of FF-DMTS with sampling times of 5, 10, 20, 30, and 60 minutes. .

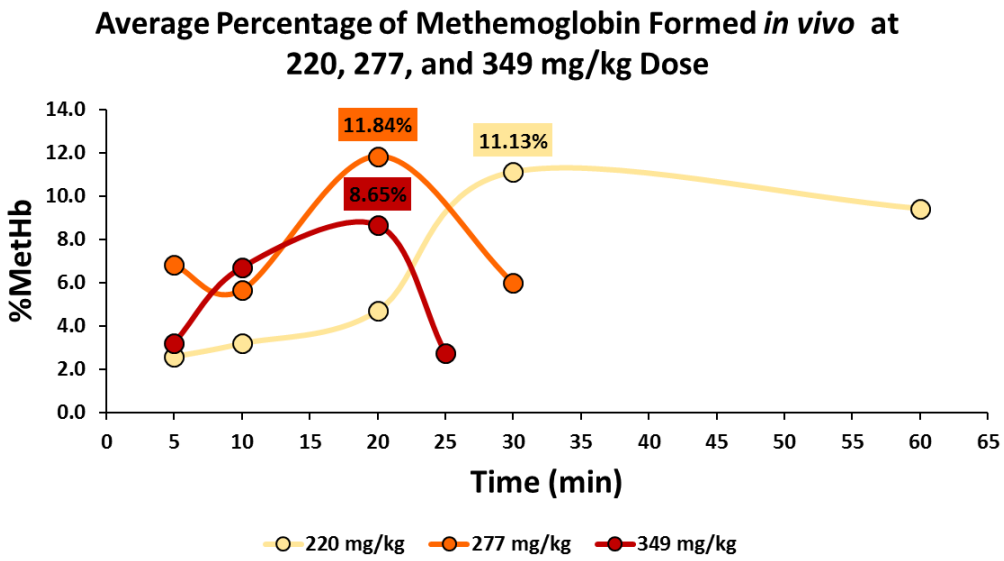

Figure 20. "High Dose" Data Set for MetHb Formation after IM injection of FF-DMTS with sampling times of 5, 10, 20, 30, and 60 minutes.

For the "low dose," the highest percentage of MetHb formed was 14.32%, which was seen at 20 minutes for the 175 mg/kg FF-DMTS dose. This was followed by the 100 mg/kg FF-DMTS dose at 30 minutes with a MetHb percentage of 8.56% and the 25 mg/kg FF-DMTS dose at 30 minutes with a MetHb percentage 2.2%. The time of maximum concentration (t_{max}) and maximum concentration (c_{max}) are directly proportional to the FF-DMTS dose (Table 6).

For the "high dose," the highest percentage of MetHb formed, which was 11.8%, was surprisingly seen in the 277 mg/kg FF-DMTS dose at 20 minutes. This was then followed by the 11.13% formed at 30 minutes for the 220 mg/kg FF-DMTS, and the 8.7% formed at 20 minutes for the 349 mg/kg FF-DMTS.

Table 6

MethHb Formation Evaluation of FF-DMTS after IM Injection in a Mice Model

FF-DMTS Dose	c_{max}	t_{max}
25 mg/kg	2.24 %	20 minutes
100 mg/kg	8.56 %	30 minutes
175 mg/kg	14.32 %	30 minutes
220 mg/kg	11.13 %	30 minutes
277 mg/kg	11.84 %	20 minutes
349 mg/kg	8.65 %	20 minutes

Table 7

MethHb Formation Evaluation of Poly 80-DMTS after IM Injection in a Mice Model

Poly 80- DMTS Dose	c_{max}	t_{max}
50 mg/kg	3.28 %	20 minutes
100 mg/kg	6.12 %	25 minutes
200 mg/kg	9.69 %	25 minutes
250 mg/kg	10.76 %	30 minutes

An initial hypothesis expected a positive correlation between the FF-DMTS dose injected IM and the % MetHb formed. The “low dose” data set supports this hypothesis; however, the %MetHb formed in the “high dose” data set is relatively lower than expected. A potential cause for this result could be due to the multiple injections needed to reach the required “high doses.” Since these injection volumes calculated for this experiment exceeded the allowed 50 µL per injection site, therefore they were divided into two separate injections into two legs. This process could potentially affect the absorption rate, thus skewing the results. In addition, at the 349 mg/kg dose, seizures were observed 5 to 10

minutes post-injection. These seizures present an additional factor in affecting the absorption rate of DMTS.

When compared to its Poly 80-DMTS counterpart (Table 7) the FF-DMTS formulation produced more MetHb per dose. After a 10-minute incubation period, the %MetHb formation for the 50, 100, 200 and 250 mg/kg doses for Poly 80-DMTS were 2.63, 4.50, 6.69 and 7.85%, respectively. The highest %MetHb formation (3.28, 6.12, 9.69 and 10.76% MetHb) was observed at 20, 25, 25 and 30 min., following IM injection of 50, 100, 200 and 250 mg/kg Poly 80-DMTS, respectively.

The production of MetHb is an important secondary antidotal pathway for DMTS, so observing this is vital for developing a useful therapeutic agent. In these studies, the formation of MetHb from both formulations was shown to be just below the levels that would require medical intervention. Neither of the formulations at the observed doses produced a c_{max} higher than 30%, which is the percentage of MetHb in the body that would require medical attention.[29]

CHAPTER IV

Conclusion

CN is a toxic cytochrome c oxidase inhibitor that prevents the production of ATP, which can result in many toxic effects such as lactic acidosis and death. DMTS is a promising SD type cyanide antidote that can react with CN to form the less toxic SCN. These studies serve to provide more insight on the characterization and biological effects of FF-DMTS as compared to Poly 80-DMTS. These two formulations are characterized using various analytical methods as described above.

In conclusion, when comparing the SD efficiencies between DMTS and TS at various pH values, in the presence and absence of Rh, it was determined that DMTS is a much more effective than TS, thus making it a prospective CN antidote alternative. In addition, when comparing the BBB penetrability of the two DMTS formulations *in vitro* using the PAMPA system, it was determined that the Poly 80-DMTS formulation (P_{app}=12.0x10^{-6} cm/s) penetrated the BBB slightly faster than the FF-DMTS formulation (P_{app}=7.5x10^{-6} cm/s).

Next, when analyzing the formation of methemoglobin by DMTS over time *in vivo* using CD-1 male mice models, the FF-DMTS produced significantly more MetHb than its Poly 80-DMTS counterpart. Up to the FF-DMTS dose of 175 mg/kg, which had the highest amount of MetHb formed (14% MetHb), there was a linear trend that was synonymous with the Poly 80-DMTS trend, which had the highest amount of MetHb formed (10% MetHb) at the 250 mg/kg dose. Although, FF-DMTS produced much more MetHb, both formulations produced less than 30% MetHb, which is the percentage of MetHb that would require medical assistance.

Lastly, when observing the particle size distribution of the two formulations using dynamic light scattering, the particle size of the FF-DMTS was over 3.5 times higher than that of the Poly 80-DMTS formulation, which can explain the slower BBB penetrability of the FF-DMTS formulation.

These data and information obtained from these studies will be used for further understanding of the antidotal effects of DMTS. Understanding how DMTS behaves in the body will give more insight into developing an adequate CN therapeutic agent alternative. By obtaining the information from these studies, we will be closer to developing an intramuscular injector kit. This approach can potentially decrease the lives lost due to CN intoxication.

REFERENCES

1. Petrikovics, I.; Budai, M.; Kovacs, K.; Thompson, D. E. Past, Present and Future of Cyanide Antagonism Research: From the Early Remedies to the Current Therapies. *World. J. Methodol.* **2015**, *5* (2), 88–100
2. Keilin D.; Hartree E. F. Cytochrome and Cytochrome Oxidase *Proc. R. Soc. Lond. B Biol. Sci.*, Cambridge, United Kingdom, February 2, 1939 127:167–191. doi: 10.1098/rspb.1939.0016
3. Way, J. L. Cyanide Intoxication and Its Mechanism of Antagonism. *Annu. Rev. Pharmacol. Toxicol.* **1984**, *24*, 451–481
4. Baskin, S. I.; Horowitz, A. M.,; Nealley, E. W. The Antidotal Action of Sodium Nitrite and Sodium Thiosulfate Against Cyanide Poisoning. *The Journal of Clinical Pharmacology*, **1992**, 32(4), 368–375
5. Rockwood, G. A.; Thompson, D. E.; Petrikovics, I. Dimethyl Trisulfide: A Novel Cyanide Countermeasure. *Toxicol. Ind. Health* **2016**, *32* (12), 2009–2016
6. Bebarta, V.S.; Tanen, D.A.; Lairet, J.; Dixon, P.S.; Valtier, S.; Bush, A. Hydroxocobalamin and Sodium Thiosulfate Versus Sodium Nitrite and Sodium Thiosulfate in the Treatment of Acute Cyanide Toxicity in a Swine (Sus scrofa) *Model. Ann Emerg Med*. **2010**, 532-538
7. Marraffa, J. M.; Cohen, V.; Howland, M. A., Antidotes for toxicological emergencies: A practical review. *American Journal of Health-System Pharmacy*, **2012,** 69(3), 199–212
8. Lang S. Uber die Umwandlung des Acetonitrils und seiner homologen im Thierkörper. Naunyn- Schmeidebergs. Arch Pathol Pharmakol. **1894**, 34:247-258

9. Block, E.; Ahmad, S.; Catalfamo, J.L.; et al. The chemistry of alkyl thiosulfonate esters. Antithrombotic 2014 Toxicology and Industrial Health 32(12) organosulfur compounds from garlic: structural, mechanistic, and synthetic studies. *Journal of the American Chemical Society*, **1986**, 108(22): 7045–7055
10. Isom, G. E.; Borowitz, J. L.; Mukhopadhyay, S., Sulfurtransferase Enzymes Involved in Cyanide Metabolism. *Comprehensive Toxicology*, **2010**, *485–500.*
11. Sörbo, B. H. [43] Rhodanese. *Methods in Enzymology*, **1955**, *334–337.* doi:10.1016/s0076-6879(55)02207-6
12. Westley, J. [37] Thiosulfate: Cyanide sulfurtransferase (Rhodanese). *Detoxication and Drug Metabolism: Conjugation and Related Systems*, **1981** *285–291.* doi:10.1016/s0076-6879(81)77039-3
13. Daneman, R.; Prat, A. The Blood–Brain Barrier. *Cold Spring Harbor Perspectives in Biology*, **2015**, 7(1), a020412
14. Gupta, S.; Dhanda, S.; Sandhir, R. Anatomy and physiology of blood brain barrier. *Brain Targeted Drug Delivery System*, **2019**, 7–31. doi:10.1016/b978-0-12-814001-7.00002-0
15. Di, L.; Kerns, E. H.; Fan, K.; McConnell, O. J.; Carter, G. T. High throughput artificial membrane permeability assay for blood–brain barrier. *European Journal of Medicinal Chemistry*, **2013**, 38(3), 223–232. doi:10.1016/s0223-5234(03)00012-6
16. Kiss, L.; Bocsik, A.; Walter, F. R.; Ross, J.; Brown, D.; Mendenhall, B. A.; Petrikovics, I. In Vitro and In Vivo Blood Brain Barrier Penetration Studies with the Novel Cyanide Antidote Candidate Dimethyl Trisulfide in Mice. *Toxicological*

Sciences, **2017**, 160(2), 398–407. doi:10.1093/toxsci/kfx190

17. Kansy, M.; Senner, F.; Gubernator, K. Physicochemical High Throughput Screening: Parallel Artificial Membrane Permeation Assay in the Description of Passive Absorption Processes. *Journal of Medicinal Chemistry*, **1998**, 41(7), 1007–1010. doi:10.1021/jm970530e
18. Sugano, K. Artificial Membrane Technologies to Assess Transfer and Permeation of Drugs in Drug Discovery. *Comprehensive Medicinal Chemistry II*, **2007**, 453–487. doi:10.1016/b0-08-045044-x/00136-x
19. Hewa Rahinduwage, C. C. Analytical method development for cyanide antidotes and characterization of a new formulation of dimethyl trisulfide. M.S. Thesis, Sam Houston State University, Hunstville, TX, 77340 https://hdl.handle.net/20.500.11875/2669 (accessed 2019-06-01)
20. Malvern Panalytical, Knowledge Center, Whitepapers. *A basic guide to particle characterization.* Malvern Panalytical, 2020 https://www.malvernpanalytical.com/en/learn/knowledge-center/whitepapers/WP120620BasicGuidePartChar (accessed 2020-03-01)
21. Malvern Panalytical, Zetasizer Nano User Manual, Malvern Panalytical, 2013. https://www.malvernpanalytical.com/en/learn/knowledge-center/user-manuals/MAN0485EN)
22. Dong, X; Kiss, L; Petrikovics, I; Thompson, D, Reaction of Dimethyl Trisulfide with Hemoglobin, *Chem. Res. Toxicol.*, **2017**, 30, 1661-1663
23. Kiss, M.; Petrikovics, I.; Thompson, D. E. Methemoglobin Forming Effect of Dimethyl Trisulfide in Mice. Hemoglobin, *International Journal for Hemoglobin*

Research, ***2018***, 42(5-6), 315–319. doi:10.1080/03630269.2018.1553182

24. Voet. D.; Voet, J.G.; Pratt, C.W. Protein function: myoglobin and hemoglobin, muscle contraction, and antibodies. In *Fundamentals of Biochemistry: Life at the Molecular Level,* 5th ed. John Wiley & Sons, 2016;pp 190–196
25. Kovacs, K.; Duke, A. C.; Shifflet, M.; Winner, B.; Lee, S. A.; Rockwood, G. A.; Petrikovics, I. Parenteral dosage form development and testing of dimethyl trisulfide, as an antidote candidate to combat cyanide intoxication. *Pharmaceutical Development and Technology*, **2016**, 22(8), 958–963
26. Hopkins, E.; Sharma, S. Physiology, Acid Base Balance, In *StatPearls*, StatPearls Publishing, 2020; https://www.ncbi.nlm.nih.gov/books/NBK507807/
27. Tayefi-Nasrabadi, H.; Rahmani, R. Partial Purification and Characterization of Rhodanese from Rainbow Trout (Oncorhynchus mykiss) Liver. *The Scientific World Journal*, **2012**, 2012, 648085
28. Abbott, N.; Rönnbäck, L., Hansson, E. Astrocyte–endothelial interactions at the blood–brain barrier. Nat Rev Neurosci, 2006 7, 41–53.)
29. Price, D. Methemoglobinemia. In: Goldfrank LR, Flomenbaum NE, Lewin NA, Weisman RS, Howland MA, Hoffman RS, eds. Goldfrank's Toxicologic Emergencies. 6th ed. Old Tappan, NJ: Appleton & Lange; **1998**, 1507-1523

APPENDIX

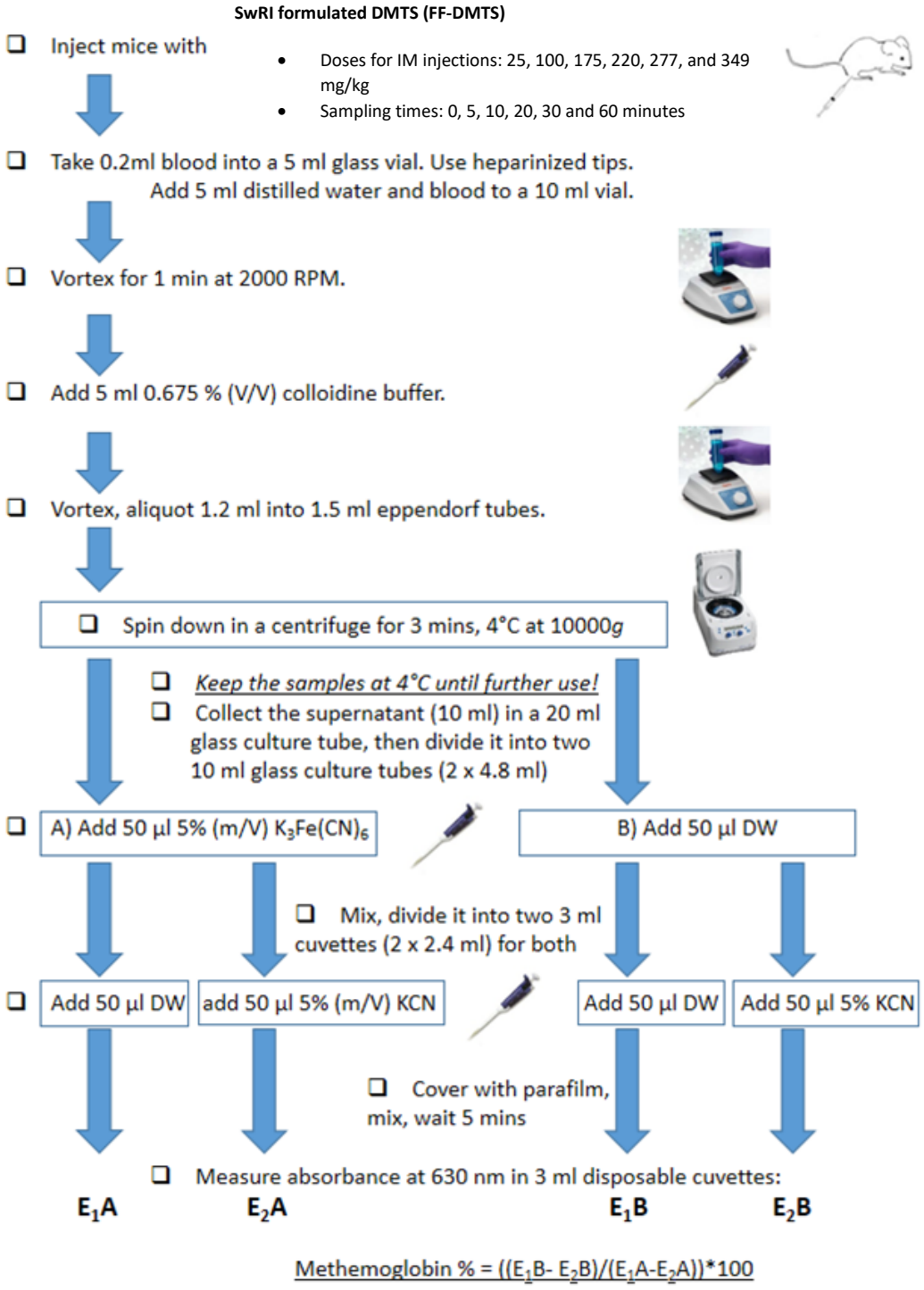

Figure A1. Schematic for MetHb Study Protocol

VITA

Christian T. Rios

EDUCATION

Sam Houston State University, Huntsville, TX
M.S. in Chemistry **August 2020**
Thesis title: "*In Vivo* and *In* Vitro Characterization of Different Dimethyl Trisulfide Formulation"

Sam Houston State University, Huntsville, TX
B.S. in Chemistry (ACS-Certified) **August 2018**
Minor in Biology

RESEARCH EXPERIENCE

Sam Houston State University, Huntsville, TX
Graduate Research Assistant **Spring 2017 – Present**
Advisor: Dr. Ilona Petrikovics

PUBLICATIONS AND PRESENTATIONS

Rios, C.T.S., Vergara, M.N., Ebrahimpour, A., Kiss, M., Warnakula, I.K., Gaspe Ralalage, R.D., Hewa R, C.C., Barrera, I., Petrikovics, I., *In vitro and in vivo characterization of the cyanide antidote SDX6F2,* ACS South West Regional Meeting, October 29- November 01, **2017**, Lubbock, Texas (Abstract # 2821909).

Warnakula, I.K., Kiss, M., Rios, C.T.S., Vergara, M., Gaspe Ralalage, R.D., Barcza, T., Petrikovics, I., *Redox reactions with dialkyl polysulfides*. ACS South West Regional Meeting, October 29- November 01, **2017**, Lubbock, Texas (Abstract # 2821927).

Gaspe Ralalage, R.D., Hewa R, C.C., Warnakula I.K., Rios, C.T.S., Kiss, M., Roy, R.J., Baca, W., Ebrahimpour, A., Petrikovics, I., *Comparision of three different cyanide antidote candidate sulfur donor molecules in vitro and in vivo*, ACS South West Regional Meeting, October 29- November 01, **2017**, Lubbock, Texas (Abstract # 2821922).

Indika K. Warnakula, Afshin Ebrahimpour, Márton Kiss, Chaturanga C. Hewa R, Christian T. Rios, Ramesha D. Gaspe Ralalage, Gary A. Rockwood, Ilona Petrikovics., *Storage Stability Studies with the Formulated Cyanide Antidote Dimethyl Trisulfide (IM-DMTS),* 57th SOT Annual Meeting, March 11-15, **2018**, San Antonio, TX. (Abstract #: 2304, Board #: P649).

Kiss, M., Sipos, P., Warnakula, I.K., Vergara, M., Rios, C.T., Whiteman, A., Gaspe R., R.D., Rockwood, G.A., Petrikovics, I. *Developing and Testing a New Intramuscular Formulation for the Cyanide Antidote Dimethyl Trisulfide*. 57th SOT Annual Meeting, March 11-15, **2018**, San Antonio, TX. (Abstract #: 2291, Board #: P636).

Kiss, M, Sipos, P, Warnakula, I.K, Whiteman, A, Rios, C.T, Upadhyaya, J, Barrera, I, Ralalage, R.D.G, Rockwood, G.A, Petrikovics, I. *In Vivo Testing of the a Novel Tricomponent-Microemulsion-Formulated Cyanide Antidote, Dimethyl Trisulfide*. 21st Biannual Medical Defense Bioscience Review **2018**, May 1-3, US Army Medical Research Institute of Chemical Defense, Aberdeen Proving Ground, MD.

Rios CTS, Vergara MN, Rodriguez LR, Upadhayaya J, Gaspe Ralalage RD, Ebrahimpour A, Whiteman AC, Kiss M, Petrikovics I. *Blood-brain Barrier Penetration of a Newly Developed, Nonaqueous Formulation of the Cyanide Antidote Candidate Dimethyl Trisulfide After Intramuscular Injection*. ACS Regional Meeting. Little Rock, Arkansas, November, **2018**. (Abstract ID: 3059290).

Vergara MN, Whiteman AC, Rios CTS, Rodriguez LR, Warnakula IK, Upadhayaya J, Ebrahimpour A, Kiss M, Petrikovics I. *Absorption of a Newly Developed, Nonaqueous Formulation of the Cyanide Antidote Candidate Dimethyl Trisulfide in Blood After Intramuscular Injection*. ACS Regional Meeting, Little Rock, Arkansas. November, **2018**. (Abstract ID#: 3059284).

Vergara MN, Rodriguez LR, Rios CTS, Whiteman AC, Kiss M, Petrikovics, I. *Absorption kinetics and brain distribution studies with the newly formulated cyanide antidote, dimethyl trisulfide, in mice*. UTSA, College of Science, "Research in Service for Better Tomorrow" San Antonio Texas, October, **2018**. (Poster #: 160).

Warnakula, I.K., Kiss, M., Rios, C.T., Vergara, M., Gaspe Ralalage, R.D., Whiteman, A.C., Petrikovics, I. *Storage Stability Studies with the SwRI Formulated Cyanide Antidote Dimethyl Trisulfide*, Texas Academy of Science Meeting, March 2-4, **2018**, Midland, Texas. (Abstract 020.158).

Rios, C.T., Ebrahimpour, A., Kefer, E., Carpenter, M., Kiss, L., Whiteman, A.C. Kiss, M., Thompson, D., Petrikovics, I. *Partitioning and Elimination Kinetics of the Cyanide Antidote Candidate Dimethyl Trisulfide in Sheep Blood*. 58th SOT Annual Meeting, Baltimore, MD. March 10-14, **2019**. (Abstract Number/Poster Board number: 2176/P577).

Gommonit, Munchelou M., Warnakula, Indika K. Rios, Christian T., Whiteman, Ashley C., Gaspe Relalage, Ramesha D., Thompson, David E., Kiss, Marton, Rockwood, Gary, Petrikovics, Ilona. *In vitro Degradation and In vivo Biotransformation of the Cyanide Antidote Candidate Dimethyl Trisulfide*. 59th SOT Annual Meeting, Anaheim, CA. March 15-19, **2020**. (Abstract Number/Poster Number: 2643/P242).

TEACHING EXPERIENCE

Sam Houston State University, Huntsville, TX

Inorganic and Environmental Chem Lab Teaching Assistant **Fall 2016**
Instructed dry and wet labs, graded lab reports, and held weekly tutoring sessions.
Supervisor: Dr. Melanie Rose and Hemantha K.Siyambalagoda

General Chemistry I Laboratory Teaching Assistant **Fall 2017**
Instructed dry and wet labs, graded lab reports, and held weekly tutoring sessions.
Supervisor: Dr. Christopher M. Zall

General Chemistry II Teaching Assistant **Summer 2015 – Spring 2020**
Instructed dry and wet lab, graded student lab reports, and held weekly tutoring sessions
Supervisor: Dr. Adrian Villalta-Cerdas

Instrumental and Analytical Chemistry Teaching Assistant **Fall 2018**
Instructed dry and wet labs using various instruments such as: UV-Vis, Fluorescence, GC-FID, GC-MS, ICP-AES, and AAS
Supervisor: Dr. David Thompson

Organic Chemistry II Teaching Assistant **Summer 2019**
Instructed dry and wet labs, graded student lab reports, and held weekly tutoring sessions
Supervisor: Dr. Christopher Hobbs

WORK EXPERIENCE

Sam Houston State University, Huntsville, TX

Stockroom Assistant **Fall 2015 – Spring 2020**
Assisted in organizing equipment, recording inventory of various reagents, disposing of chemical waste, and maintaining cleanliness of labs
Supervisor: Dr. Rukma Basnayake

Sam Houston State University, Huntsville, TX
General Chemistry II Chemical Prep **Summer 2015 – Summer 2020**
Prepared and kept inventory of all the reagents and solutions that were necessary to run the General Chemistry II labs
Supervisor: Dr. Rukma Basnayake

Sam Houston State University, Huntsville, TX
Organic Chemistry II Chemical Prep **Summer 2017 – Summer 2020**
Prepared and kept inventory of all the reagents and solutions that were necessary to run the Organic Chemistry II labs
Supervisor: Dr. Rukma Basnayake

AWARDS

Excellence in Writing Recognition **Fall 2015**
Enhancing Undergraduate Research Experiences and Creative Activities Grant **Fall 2017**
Research Fellowship, Robert A. Welch Foundation **Spring 2017**
The Sammy Award Nomination **Spring 2018**
College of Science and Engineering Technology Graduate Recruitment Scholarship **Fall 2018 – Spring 2019**
College of Science and Engineering Technology Graduate Achievement Scholarship **Spring 2020**
The Graduate School at Sam Houston State University Travel Fund **Spring 2019-Spring 2020**

COLLABORATIVE INSTITUTIONAL TRAINING INITIATIVE CERTIFICATIONS

Reducing Pain and Distress in Laboratory Mice and Rats
Using Hazardous and Toxic Agents in Animals
Working with Mice in Research Settings
Working with Rats in Research Settings
Working with the IACUC
RCR for Social, Behavioral, and Education (SBE) Sciences
CITI Conflicts of Interest

MEMBERSHIPS AND ASSOCIATIONS

Tri-Beta National Biological Honors Society - Treasurer
Sam Houston Association of Medically Oriented Students – Fundraising Chair
American Chemical Society J.C. Stallings Chemical Society
Society for the Advancement of Material and Process Engineering

SKILLS AND EXPERIENCE

Biochemistry and Small animal models
Characterization using GC-MS, GC-FID, HPLC, Zetasizer, and UV-Vis
Software experience with Gaussian09W
Proficiency in Microsoft Word, Excel, and PowerPoint
Experience using Python